



Contents lists available at ScienceDirect

Arabian Journal of Chemistry

journal homepage: www.ksu.edu.sa

Original article

Design and synthesis of chitosan/calcium lignosulfonate/Au NPs: Its performance for reduction of nitro compounds and in the treatment of cancer



Ruyi Xie^a, Jianming Zhou^a, Ting Wang^a, Yuan Xu^b, Bei Zhang^{a,*}, Sally Negm^c, Attalla F. Elkott^{d,e}

^a Gastroenterology Department, The 2nd Affiliated Hospital of Nanchang University, Jiangxi 330006, China

^b Information Department, The 2nd Affiliated Hospital of Nanchang University, Jiangxi 330006, China

^c Department of Life Sciences, College of Science and Art Maheyel Aseer, King Khalid University, Abha 62529, Saudi Arabia

^d Department of Biology, College of Science, King Khalid University, 61421 Abha, Saudi Arabia

^e Department of Zoology, Faculty of Science, Damanhour University, Damanhour 22511, Egypt

ARTICLE INFO

Keywords:

Chitosan
Lignosulfonate
Gold nanoparticles
Cancer
MTT assay

ABSTRACT

This work introduces the preparation of a novel type of crosslinked polymers support based on calcium lignosulfonate-chitosan (CLS-CS) hydrogel with capping/reducing ability to encapsulated gold nanoparticles (CLS-CS/Au NPs). The morphology, structure and physicochemical properties of the prepared nanoparticles were characterized by different analytical techniques such as FT-IR, FE-SEM, TEM, EDX-elemental mapping study. The obtained results shown that CLS-CS/Au NPs prepared as spherical particles with sizes of 20–30 nm. The CLS-CS/Au NPs was applied as well for reduction of nitroarenes. The reduction of nitroarenes was obtained with good to high yields within short times. The related nanocatalyst was recovered for eight runs without significant loss of its catalytic performance. The MTT examination was conducted to check the anti-pancreatic cancer, anti-gastric cancer, anti-colorectal carcinoma, and cytotoxicity efficacies of the treated cells with CLS-CS/Au NPs over a 48-hour period on normal (HUVEC) and cancer cells. The IC₅₀ values of the CLS-CS/Au NPs were found to be 169 µg/mL for HT-29 (colorectal carcinoma cell), 196 µg/mL for MKN45 (Gastric cancer cell), and 112 µg/mL for PANC-1 (Pancreatic cancer cell). The growth of malignant colorectal, gastric and pancreatic cells was found to decrease in a dose-dependent manner when exposed to CLS-CS/Au NPs. Following clinical research, CLS-CS/Au NPs shows promise as an effective treatment for colorectal, gastric and pancreatic cancers.

1. Introduction

The complexities and interconnections behind the clinical trials failure to achieve the desired multifaceted outcomes are evident. Regrettably, therapeutic agents such as nanotechnology, biology, and chemotherapy exhibit remarkable selectivity and efficacy in targeting cancer cells in animal and even *in vitro* models. Nonetheless, the failure in clinical trials is not an absolute norm but rather an exception (Itani and Al Faraj, 2019; Trojer et al., 2013; Liu et al., 2014; Gao et al., 2015). This is primarily due to the therapeutic agents' intricate biological distribution, which can significantly impact the outcome. Inadequate concentration at non-targeted sites and excessive concentration at unintended locations can result in dose-limiting toxicity (Trojer et al.,

2013; Liu et al., 2014; Gao et al., 2015). Despite extensive efforts in pharmaceutical companies and laboratories over the past 30 years, the adding targeting sections strategy to therapeutic nanoparticles to ameliorate location specification has not yet resulted in clinically approved drugs (Mohammed et al., 2016; Li and Gu, 2014; Yang et al., 2011). This lack of success can be attributed to the fact that while the molecular agents addition enhances cognitive targeting characteristics, it also presents significant challenges in managing biological barriers (Li and Gu, 2014; Yang et al., 2011; Xinli, 2012; Allen, 2002).

Various countries have different definitions of nanotechnology, leading to variations in the clinical validation of nanodrugs. Despite these differences, the common denominator among these definitions is the utilization of nanoscale structures. The application of

* Corresponding author.

E-mail address: beibe3030@sina.com (B. Zhang).

<https://doi.org/10.1016/j.arabjc.2024.105709>

Received 23 January 2022; Accepted 3 March 2024

Available online 5 March 2024

1878-5352/© 2024 Published by Elsevier B.V. on behalf of King Saud University. This is an open access article under the CC BY-NC-ND license (<http://creativecommons.org/licenses/by-nc-nd/4.0/>).

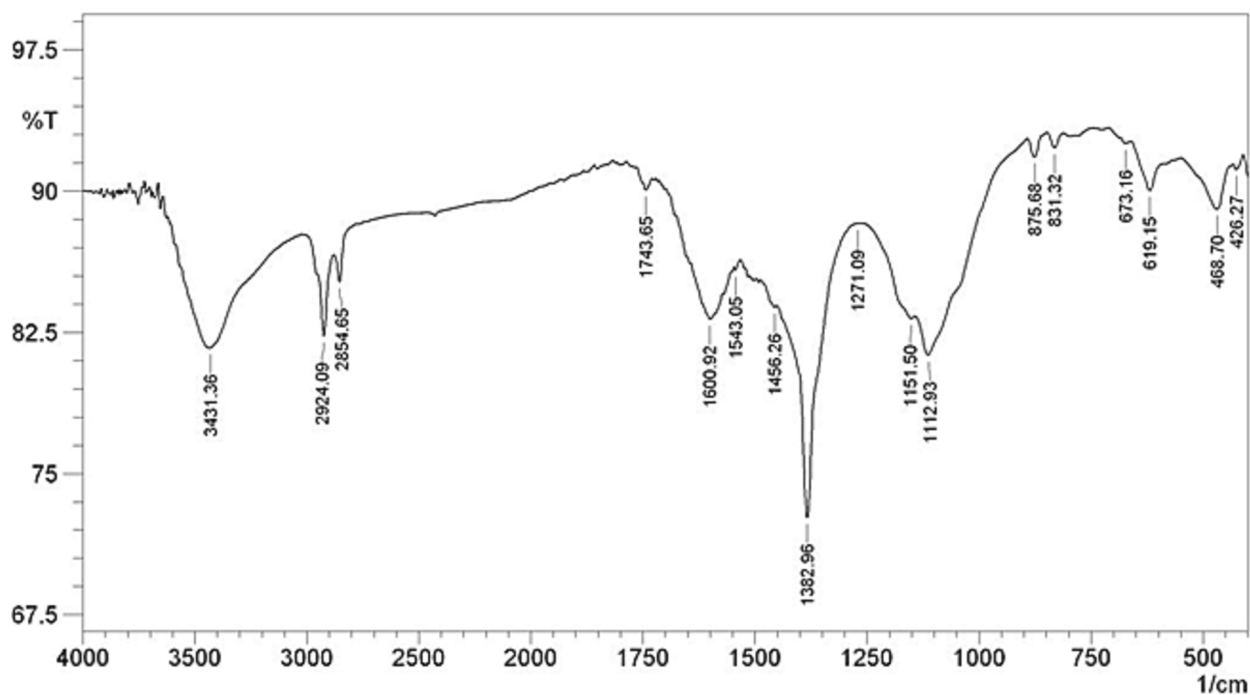


Fig. 1. FT-IR spectrum of CLS-CS/Au NPs.

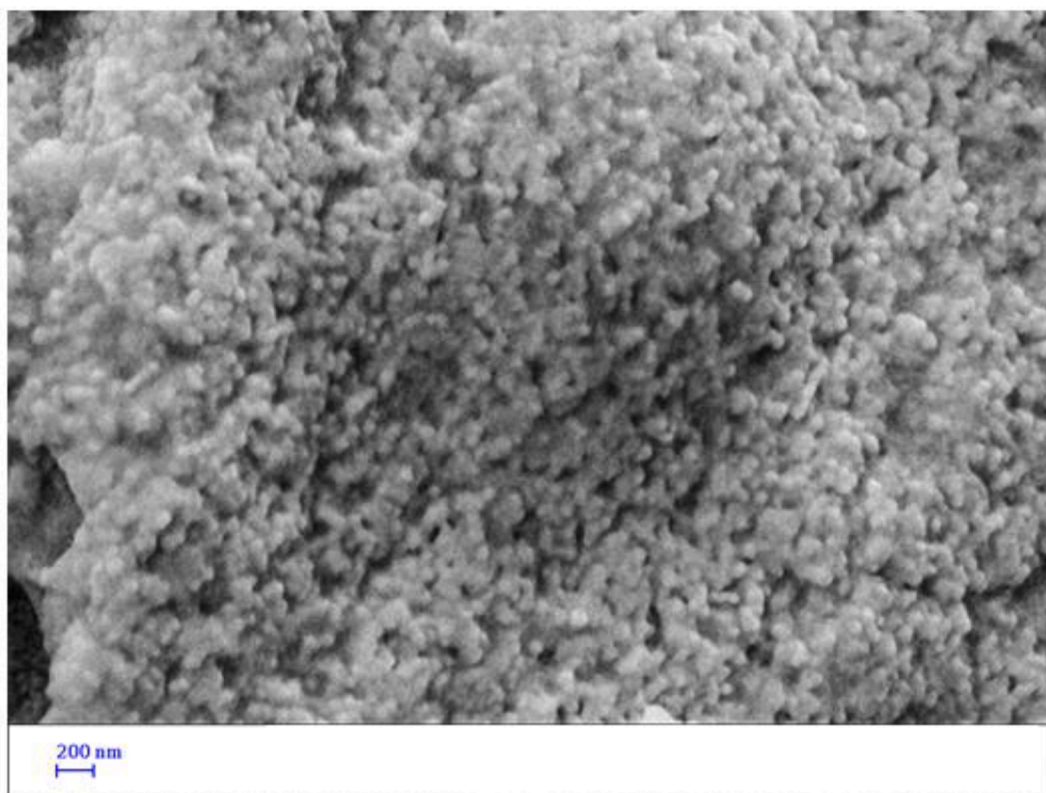


Fig. 2. FE-SEM image of the CLS-CS/Au NPs.

nanotechnology in disease treatment offers numerous advantages (Abbasi et al., 2021; Ma et al., 2020; Itani and Al Faraj, 2019).

Metal nanoparticles and metal oxides are commonly utilized by medical manufacturers and consumers. The toxicity induced by nanoparticles on cancer cells is primarily due to the ROS generation. ROS overproduction can result in oxidative stress, regular physiological

functions disturbance, and oxidation regulation. Consequently, these impacts can cause DNA damage, alterations in cell signaling pathways, modifications in cell growth, cytotoxicity, programmed cell death, and cell demise initiation (Allen, 2002; Abbasi et al., 2021; Ma et al., 2020; Itani and Al Faraj, 2019; Guilbert et al., 1996; Miller and Krochta, 1997).

Various factors can have a significant impact on the generation of

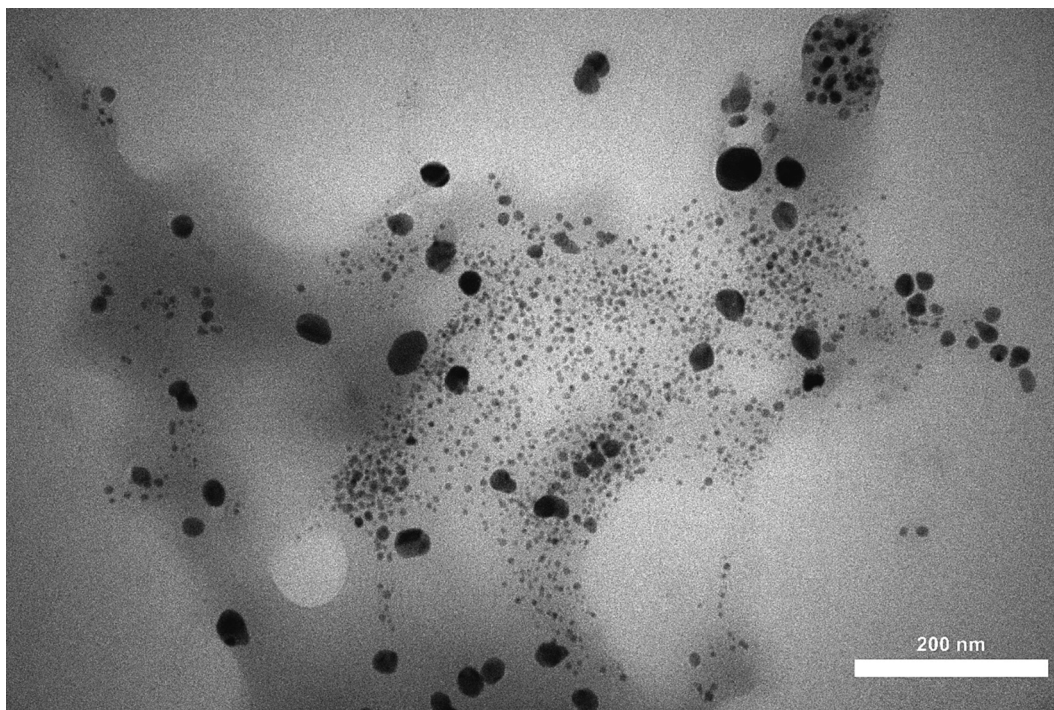


Fig. 3. TEM image of the CLS-CS/Au NPs.

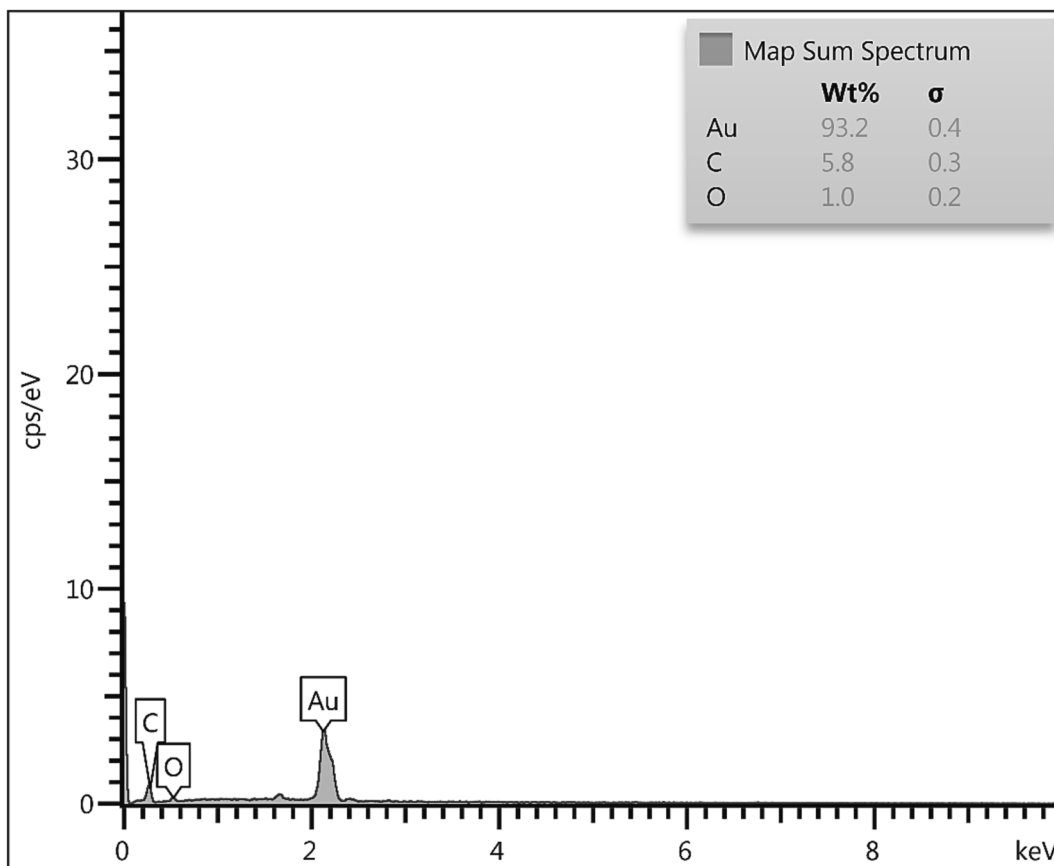


Fig. 4. EDX of the CLS-CS/Au NPs.

ROS. These factors, which are critical and deterministic in nature, encompass characteristics such as shape, size, surface area of nanoparticles, baroelectricity of particle surfaces, surface-forming groups,

solubility of particles, emission of metal ions from nanoparticles and nanomaterials, optical activation, cell reactions model, ambient pH, and inflammatory efficacies (Abbasi et al., 2021; Ma et al., 2020; Itani and Al

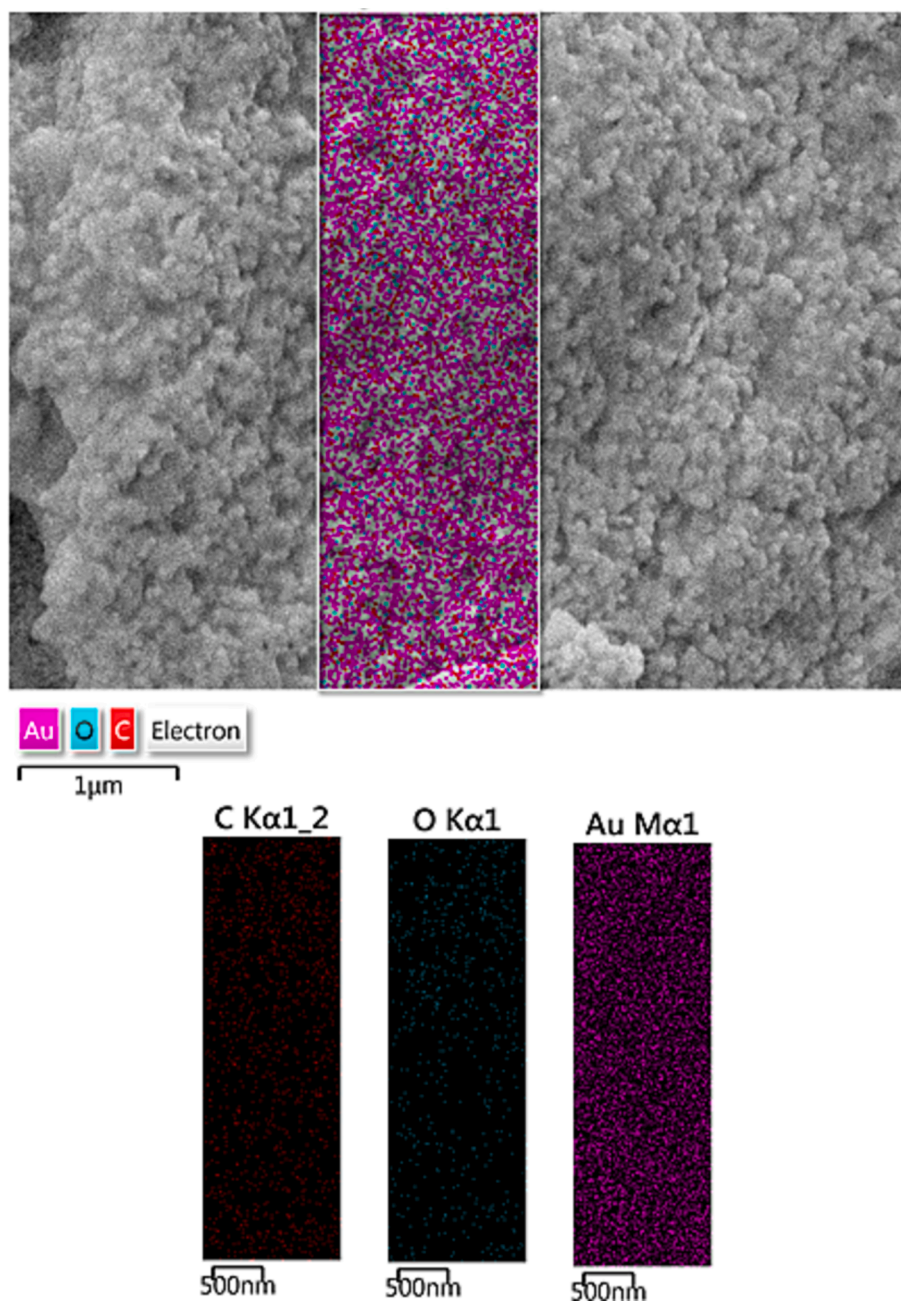


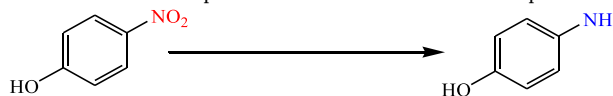
Fig. 5. Elemental mapping of CLS-CS/Au NPs.

Faraj, 2019; Guilbert et al., 1996; Miller and Krochta, 1997; Debeaufort et al., 1998).

Metal nanoparticles and metal oxide nanoparticles exhibit enhanced optical efficacies attributed to their high atomic number and large active surface area. These properties amplify the Compton and photoelectric effects during interactions with gamma-ray and X-ray radiation in diagnostic and therapeutic applications. Ultimately, these nanoparticles have the potential to advance techniques for targeting and destroying tumor cells, thereby reducing their survival rates in radiation therapy (Guilbert et al., 1996; Miller and Krochta, 1997; Debeaufort et al., 1998; Fazaeli et al., 2010; Xue et al., 2021). The strategies for preparing microenvironmental and diagnostic-therapeutic nanoparticles will undergo significant changes (Itani and Al Faraj, 2019; Guilbert et al., 1996; Miller and Krochta, 1997; Debeaufort et al., 1998).

In the past few days, there has been a growing recognition of the significance of biomolecular engineered nanoparticles as innovative

nanomedicine formulations. This is primarily due to their remarkable biocompatibility, small size that allows them to bypass cellular barriers, extensive surface area that enables efficient drug delivery with high capacity, and their ability to selectively target affected areas. Numerous studies have documented the utilization of biopolymer-coated nanoparticles or plant phytochemicals in medicinal therapeutics (Guilbert et al., 1996; Miller and Krochta, 1997; Debeaufort et al., 1998; Fazaeli et al., 2010; Xue et al., 2021; Shi et al., 2021; Huang et al., 2021; Zhao et al., 2021; Oueslati et al., 2020; Venditti, 2019; Rossi et al., 2016; Umamaheswari et al., 2018; Fratoddi et al., 2018; Aromal and Philip, 2012; Zhang et al., 2020; Shahriari et al., 2021). Au NPs, among various metal variants, have shown remarkable bioactivities such as antifungal, antioxidant, and antimicrobial efficacies on different bacteria and fungi (Zhaleh et al., 2019). Furthermore, their potential as unconventional chemotherapeutic drugs and in cancer diagnosis has been extensively investigated through *in vivo* and *in vitro* studies (Sun et al., 2019; Wu

Table 1Evaluation of reaction parameters in the reduction of 4-Nitrophenol catalyzed by CLS-CS/Au NPs.^a


Entry	Catalyst	Cat. Loading (Au mol%)	NaBH ₄ (mmol)	Time (min)	Yield (%) ^b
1	–	–	3.0	180	–
2	CS	–	3.0	180	–
3	CLS-CS	–	3.0	180	–
4	CLS-CS/Au NPs	0.20	1.0	30	75
5	CLS-CS/Au NPs	0.20	2.0	20	80
6	CLS-CS/Au NPs	0.20	3.0	10	96
7	CLS-CS/Au NPs	0.20	4.0	10	96
8	CLS-CS/Au NPs	0.30	3.0	8	96
9	CLS-CS/Au NPs	0.10	3.0	30	85

^a Condition: 4-nitrophenol (1.0 mmol) in 5 mL H₂O at r.t.^b Isolated yield.

et al., 2018; Ledari et al., 2020). Previous reports have demonstrated the impressive outcomes of bio-functionalized and modified Au NPs in *in vitro* research on several cancer cells (Singh et al., 2018).

Nitroarenes are considered as the most alarming chemical contaminants of natural and potable water. Due to unawareness of people or led by unethical business strategy, different derivatives of this moiety are being expelled by a number of chemicals, dyes, drugs, textile and paper industries into river streams or water reservoirs that pollute the dangerously (Cermakova et al., 2017; Zhou et al., 2015; Ayad et al., 2017). On consumption of this contaminated water severe damage occurs to the nervous system, kidney and liver of different living species including human (Shah et al., 2017; Veisi et al., 2021; Das et al., 2019; Veisi et al., 2019). Therefore, quenching of harmful effects of nitroarenes before disposal would be an effective solution towards the problem. So, we decide to preparation *in situ* supported Au NPs over two biomolecules chitosan-calcium lignosulphonate (CLS-CS) to make a cross-linked polymer catalyst (CLS-CS/Au NPs). These two biomolecules acted as green reducing agent for conversion of Au ions to Au NPs without using any reducing and toxic reagents. Subsequently, CLS-CS/Au NPs nanocatalyst was applied catalytically for reduction of nitroarenes by using NaBH₄ as the hydride donor. The nanocomposite material synthesized in this study has undergone characterization using various physicochemical techniques. Subsequently, it has been utilized as a chemotherapeutic drug against cell lines associated with common pancreatic, colorectal, and gastric cancers.

2. Experimental

2.1. Synthesis of the CLS-CS/Au NPs

First, equal proportions of chitosan (CS) and calcium lignosulfonate (CLS) (0.1 g each) were dissolved in 1 % acetic acid solution (50 mL) through stirring for 60 min at 25 °C to make a homogenous CLS-CS composite. Next, the pH of the reaction medium was adjusted to pH 10 and a 10 mL aqueous solution containing 0.02 g HAuCl₄ was added dropwise to the above mixture and stirred for 5 h at 80 °C. Finally, the obtained CLS-CS/Au NPs nanocomposite were collected by centrifuge and rinsed with deionized water and ethanol sequentially.

2.2. General reduction of nitroarenes catalyzed by CLS-CS/Au NPs

For this purpose, nitroarenes (1 mmol) and NaBH₄ (3 mmol) was added to deionized water (5 mL) and stirred to obtain a homogeneous solution. Next, the CLS-CS/Au NPs nanocomposite (0.2 mol% Au) was added to the solution, and the reaction was allowed to proceed for desired time at 25 °C. End of the reaction, the catalyst was separated over centrifuge and the organic layer was dried over dehydrated Na₂SO₄ and the crude products were purified by using a pad column

chromatography.

2.3. Antioxidant activities of CLS-CS/Au NPs nanocomposite

In this approach, varying concentrations of nanoparticles (ranging from 0 to 1000 µg/ml) were mixed with 1 mL of DPPH (300 µmol/l). The resulting mixture was then diluted with methanol to reach a final volume of 4000 µl. Subsequently, the samples were incubated in darkness for 1 h. The absorbance at 517 nm was measured. The DPPH radical inhibition percentage was determined by the equation (Lu et al., 2021).

$$\text{Inhibition (\%)} = \frac{\text{Sample A.}}{\text{Control A.}} \times 100$$

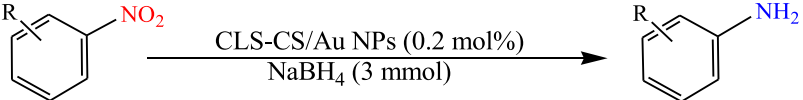
2.4. Anti-pancreatic carcinoma, anti-gastric cancer, and anti-colorectal cancer properties of CLS-CS/Au NPs

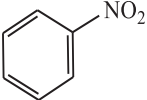
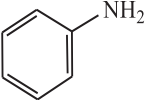
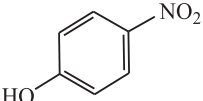
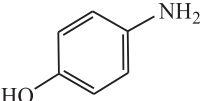
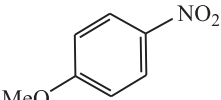
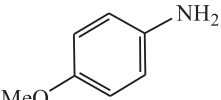
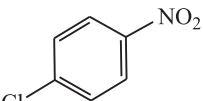
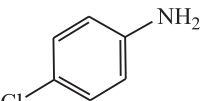
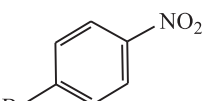
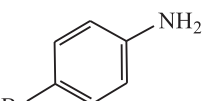
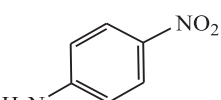
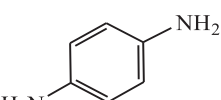
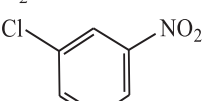
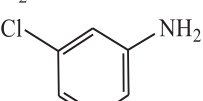
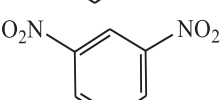
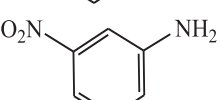
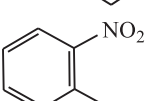
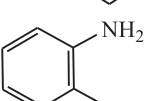
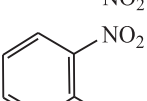
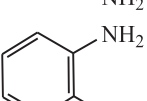
HT-29 (colorectal carcinoma cell), MKN45 (Gastric cancer cell), and PANC-1 (Pancreatic cancer cell) were used in the current research.

Cell culture involves the cultivation of eukaryotic cells in a specialized medium that provides optimal growth conditions for each cell type. To support their growth, artificial environments typically include essential nutrients like gases, hormones, amino acids, sugars, minerals, and vitamins. Additionally, the chemical and physical conditions of the environment must be carefully regulated to promote cell growth. Depending on the cell type, some cells require a surface to attach to in order to grow, while others can thrive while floating in the culture medium. In laboratory settings, specific cell culture mediums are designed to cater to the needs of particular cell types (Abbasi et al., 2021; Ma et al., 2020). To ensure optimal cell proliferation, it is important to maintain a moderate cell density in the culture medium. Regular transfer of cells to fresh medium, known as passage, should be performed every few days. If the cell volume and density raise too much, it can hinder cell proliferation and lead to cellular differentiation. The objectives of cell culture include evaluating cell growth, nutritional needs, growth arrest, and observing changes in cell morphology under a microscope. In order to investigate the cell growth cycle, control the cancer cells growth, and examine gene expression, it need to conduct cell culture outside of the organism. This allows for a more detailed analysis of the specific type of growth and cells growth rate. Cell culture also finds application in the study of animal evolution. By culturing a fertilized cell in a laboratory setting, we can explore how it develops into a multicellular organism and observe the morphological differences of each cell under a microscope. This approach enables us to understand the cell culture stages in relation to evolution (Lu et al., 2021). Within the cell culture medium, cells are prepared and undergo differentiation, giving rise to new cells with the aid of growth factors and hormones. Through the cell culture process, cells with identical characteristics are

Table 2

Generality of reduction in the presence of CLS-CS/Au NPs catalyst.^a



Entry	Substrate	Product	Time (min)	Yield (%) ^b
1			40	96
2			15	96
3			15	96
4			20	95
5			20	96
6			15	96
7			20	95
8			30	92
9			60	90
10			60	92

^a Reaction condition: nitroarenes (1.0 mmol), NaBH₄ (3 mmol), water (5 mL), CLS-CS/Au NPs (0.2 mol%).

^b Isolated yields.

generated, allowing for the study of various intracellular functions and cell metabolism. Once a molecule binds to its specific membrane receptor, subsequent intracellular reactions including the formation of complexes, intracellular messaging, and message transmission can be assessed. These cultured cells have the advantage of being able to be stored at extremely low temperatures, which helps to preserve their genetic composition and growth rate. Consequently, these cells can be utilized whenever necessary, even if it is a month later. Cell aging can be effectively prevented using this approach. When conducting studies involving animals like rats and rabbits, it is crucial to take into account animal homeostasis and experimental stress. However, when it comes to cell culture, these factors do not apply. The standardization of laboratory tests is simpler compared to studying animals, as it allows for better control over cell environments, including osmotic pressure, heat,

acidity, as well as carbon dioxide and oxygen pressures (Lu et al., 2021).

In the recent study, the cells were stored in an incubator with 5 % CO₂ at 37 °C. Once the flask was approximately 80 % filled, cell passage was conducted, and around 10⁵ cells were seeded in 24-well petri dishes under normal environmental conditions. After 24 h, the cells were treated with nanoparticles. The cultured cells' survival rate was assessed using various concentrations. For this study, cells were cultured at a density of 3 × 10⁴ cells/well in 24-well plates and placed in an incubator at 37 °C. Subsequently, the old culture medium was aspirated from the wells, and the cells were exposed to varying nanoxidro concentrations. This assessment was conducted on the 1th, 2th, and 3th days post-treatment; hence, after the appropriate incubation period in the 24-well plates, the culture medium was replaced with approximately 300 μl of new medium in each well. After an incubation period of 3–4 h at

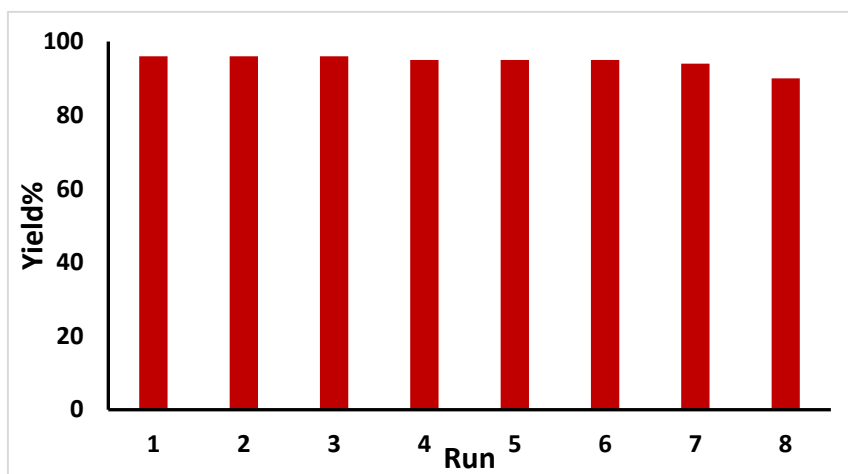


Fig. 6. Study of reusability of CLS-CS/Au NPs.

Table 3

The IC₅₀ of BHT, CLS-CS/Au NPs, and HAuCl₄ in antioxidant test.

	HAuCl ₄ (μg/mL)	CLS-CS/Au NPs (μg/mL)	BHT (μg/mL)
IC ₅₀ against DPPH	–	120 ± 0 ^a	104 ± 0 ^a

37° C, the MTT solution is aspirated and 200 μl of DMSO from Merck, USA (100 %) is added to each well. Subsequently, the samples absorbance was measured at a wavelength of 570 nm by an ELISA reader. This procedure was replicated thrice, with four wells allocated for each concentration of nano oxide. The cell viability percentage was determined using the formula (Lu et al., 2021):

$$\text{Cell viability (\%)} = \frac{\text{Sample A.}}{\text{Control A.}} \times 100$$

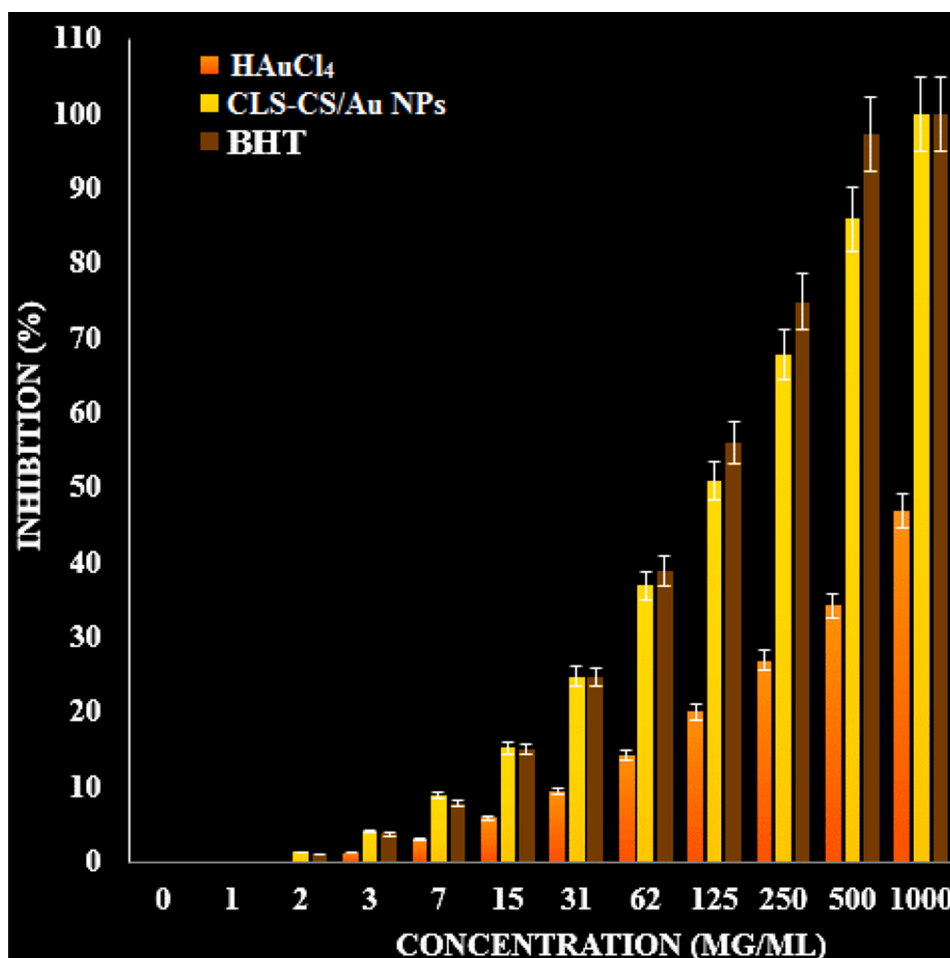


Fig. 7. The antioxidant properties of BHT, CLS-CS/Au NPs, and HAuCl₄ against DPPH.

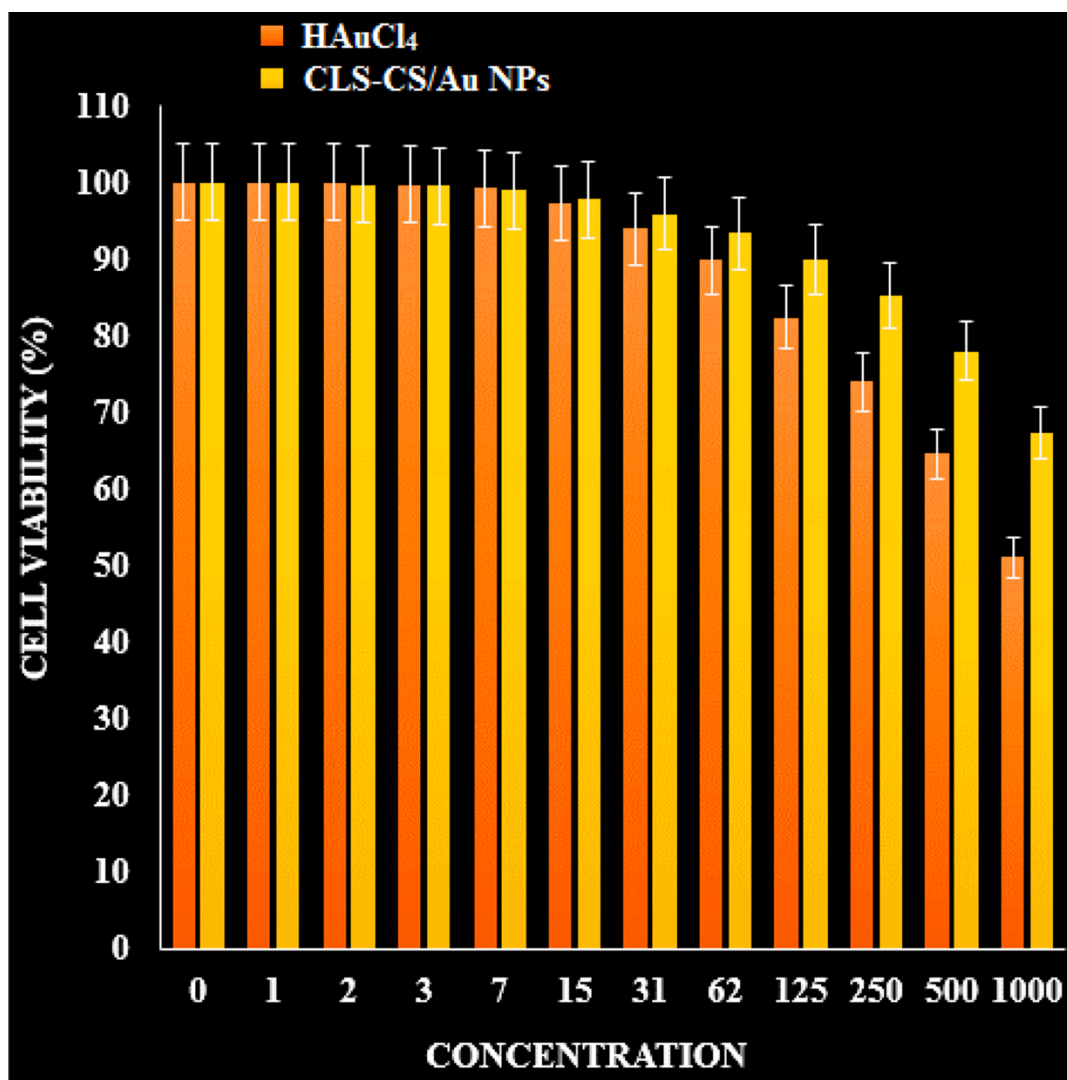


Fig. 8. The cytotoxicity effects of CLS-CS/Au NPs and HAuCl₄ on normal cell.

2.5. Statistical analysis

The Mean \pm SE was calculated for the results by SPSS-22. Statistical tests of variance were conducted using a completely randomized block design. Graphs were created in Excel software ($P < 0.05$).

3. Results and discussion

3.1. Structural study of the synthesized CLS-CS/Au NPs

The preparation of CLS-CS/Au NPs nanocomposite was described by a post-synthetic modification method based on CS and CLS, which used for *in situ* fabrication of Au NPs. The final CLS-CS/Au NPs nanocomposite was subsequently analyzed using a number of advanced techniques like FT-IR, TEM, FE-SEM, EDX-elemental mapping and ICP-OES.

To confirm the successful fabrication of CLS-CS/Au NPs nanocomposite, FT-IR analysis is recorded and presented in Fig. 1. The representative peaks of chitosan are appeared at 619, 1030–1050, 1151, 1382, 1543, 1600 and 2854–2924 cm^{-1} assigned to N–H, C–O, C–O–C, C–N, in plane N–H bending, C=O stretching and C–H stretching respectively. The broad peak observed at 3431 cm^{-1} assigned to the mixed N–H and O–H stretching vibrations. Also the presence of

CLS could be confirmed with appearance the typical peaks for SO₃ adsorption at 673 cm^{-1} , C–O stretching at 1151 cm^{-1} and O–H stretching at 3400–3500 cm^{-1} . These observations shown the well attachment of Au NPs to the CLS-CS matrix.

The microscopic structures, morphology and size distributions of the CLS-CS/Au NPs were determined by FE-SEM and TEM studies. Fig. 2 shown the FE-SEM analysis of the CLS-CS/Au NPs composite, which indicating the successful preparation of spherical Au NPs that encapsulated in the CLS-CS hydrogel layers. For further detailing regarding the particle size and their distribution, TEM analysis was performed (Fig. 3). The result presented spherical Au NPs as dark spots with an average size of 20–30 nm.

Fig. 4 presented the profile for chemical constitution of CLS-CS/Au NPs, as analyzed by EDX investigations, equipped with SEM instrument. It clearly shows Au as metallic elements as a major and broad signal at 2.1 eV. The non-metallic signals of C and O appeared at lower region are attributed to the CLS-CS functionalization coated over the surface. Next, an elemental mapping study was conducted to further extend the elemental analysis. (Fig. 5). The obtained results shows the constitutional elements and their respective positions as represented by colored dots scattered over the material surface.

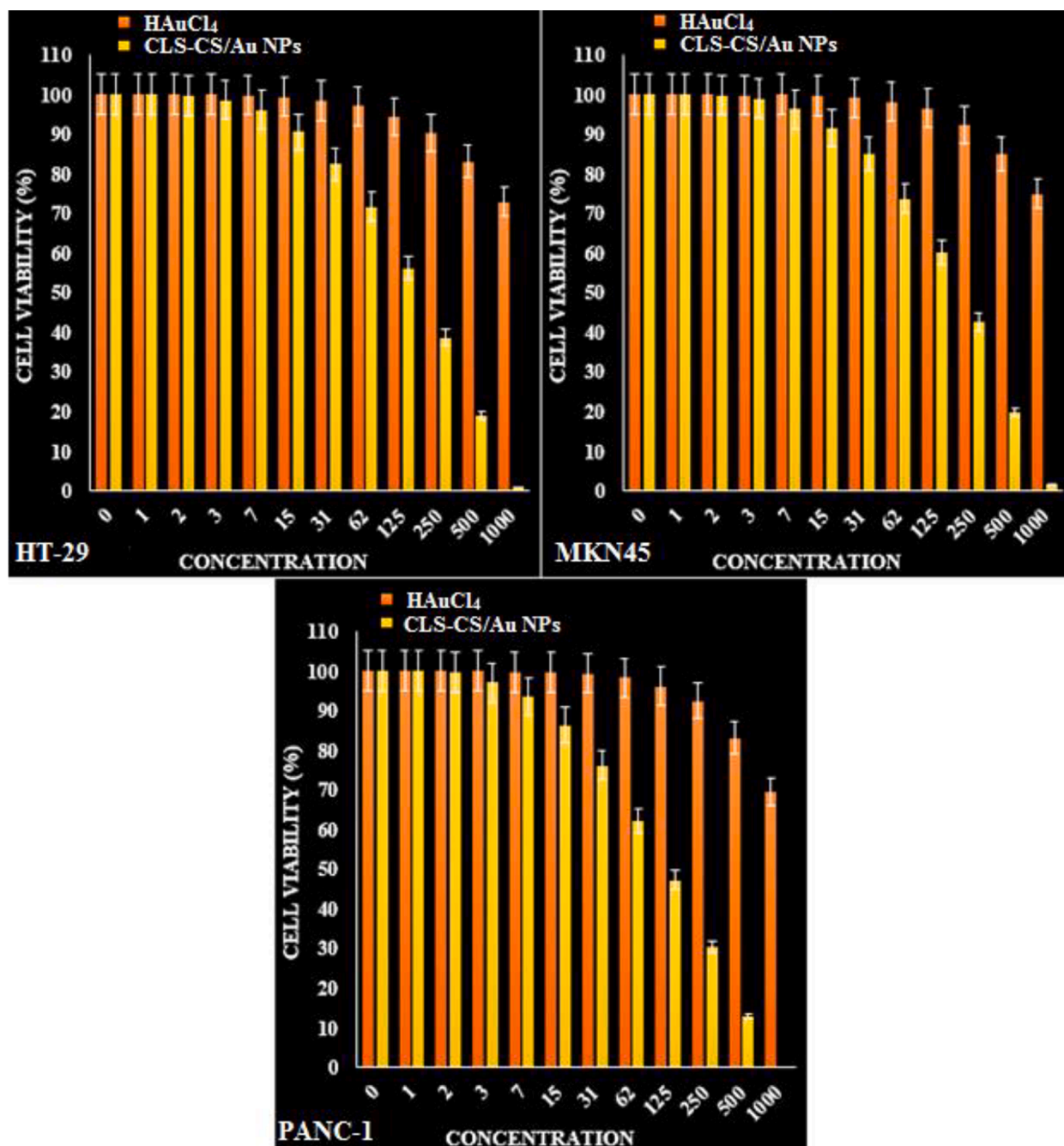


Fig. 9. The anti-cancer properties of HAuCl₄ and CLS-CS/Au NPs against SK HT-29 (colorectal carcinoma cell), MKN45 (Gastric cancer cell), and PANC-1 (Pancreatic cancer cell).

Table 4

The IC₅₀ of HAuCl₄ and CLS-CS/Au NPs in the anticancer test.

	HAuCl ₄ (µg/mL)	CLS-CS/Au NPs (µg/mL)
IC ₅₀ against HUVEC	–	–
IC ₅₀ against SK-OV-3	–	169 ± 0 ^b
IC ₅₀ against SW-626	–	196 ± 0 ^b
IC ₅₀ against PA-1	–	112 ± 0 ^a

3.2. Reduction of nitroarenes catalyzed by CLS-CS/Au NPs

After the characterization of CLS-CS/Au NPs, its catalytic performance was investigated for reduction of nitroarenes. So, to optimize the reaction conditions by choosing a model reduction involving 4-

nitrophenol and the effect of various parameters such as amount catalyst and amount of NaBH₄ were studied that presented in the Table 1. The reaction did not proceed in the absence of the catalyst, even after the use of NaBH₄ (3.0 mmol) for long time (Table 1, entry 1). However, the reaction was good using CLS-CS/Au NPs as catalyst and the best result (96 % yield) was achieved in 10 min when 0.2 mol% Au composite was applied in the presence of NaBH₄ (3.0 mmol) (Table 1, entry 6). We experimented with different amount of catalyst and NaBH₄ (Table 1, entries 7–9), but could not obtained better results than the entry 6.

After obtain the optimized conditions, its generality was investigated with a wide variety of nitroarenes having different functions (Table 2). Both the withdrawing and electron-donating groups were resulting excellent yields under the optimized protocol in short times (Table 2, entries 1–10).

The reusability of the catalyst was investigated by model reaction and shown it could reuse 8 runs without significant loss of its catalytic activity (Fig. 6).

3.3. Antioxidant effects analysis of CLS-CS/Au NPs

Metallic nanoparticles consist of various compounds, each possessing a unique structure. The compounds extraction process is influenced by various factors, with the type of extraction and solvent method being the most crucial. Selecting a suitable solvent for a specific group of metallic nanoparticles compounds can be challenging due to the presence of other substances that impact the solubility of these compounds. When extracting NPs, it is essential to utilize a method that ensures optimal preservation of antioxidant compounds. Typically, metallic nanoparticles possess distinct antioxidant properties. Recent research has indicated that when these NPs are incorporated into metal nanoparticles as reducing and stabilizing agents, they create nanocomposites with exceptional antioxidant efficacies. Antioxidants are commonly known as substances capable of delaying, decelerating, and even halting oxidation processes. They effectively safeguard against alterations in the color and food flavor caused by oxidation reactions (Beheshtkhoo et al., 2018; Sangami and Manu, 2017; Katata-Seru et al., 2018; Sankar et al., 2014). The mechanism of oxidants can be counteracted by their ability to hinder the propagation of oxidation chain reactions through the provision of hydrogen atoms to free radicals. However, the synthetic antioxidants utilization like TBHQ, BHA, BHT, and other chemical additives has been restricted in recent times due to their potential toxicity and carcinogenic properties. Presently, the primary emphasis in research within this field lies in exploring the application of novel and harmless antioxidants derived from food, microbial, animal, and plant sources (Conde et al., 2012; Riehemann et al., 2009; Rai et al., 2014; Jo et al., 2015; Bhattacharya, 2011).

Various drugs are made using metallic nanoparticles secondary metabolites. These metabolites include amino acids, flavonoids, phenols, saponins, steroids, terpenoids, and alkaloids. The production of these drugs has been successful, thanks to the presence of these metabolites (Beheshtkhoo et al., 2018; Sangami and Manu, 2017). Flavonoids, which are part of the large family of secondary metabolites, have a structural skeleton of diphenylpropane or polyphenols and including two aromatic benzene rings. Currently, there have been 6,000 different flavonoids identified, with major ones being compferrol, quercetin, and myristin. Luteolin and apigenin are the two primary flavonoids, encompassing a total of 62 distinct types that can be found in a range of fruits, vegetables, and edible tropical NPs. These flavonoids possess several well-known effects, including the ability to eliminate free radicals, inhibit certain enzymes, and exhibit anti-inflammatory effects (Beheshtkhoo et al., 2018; Sangami and Manu, 2017; Katata-Seru et al., 2018; Sankar et al., 2014). Some evidence suggests that the compounds biological impacts are linked to their antioxidant efficacy. Antioxidants function by several mechanisms within the body, such as exerting anti-inflammatory effects, inducing apoptosis, boosting the immune system, halting the cell cycle, and promoting cell differentiation (Beheshtkhoo et al., 2018; Sangami and Manu, 2017; Katata-Seru et al., 2018; Sankar et al., 2014; Namvar et al., 2014).

Table 3 and Fig. 7 present the findings of a recent study, highlighting the scavenging capacity of CLS-CS/Au NPs and BHT at various concentrations. The antioxidant test revealed that the IC₅₀ values of BHT and CLS-CS/Au NPs against DPPH free radicals were 104 and 120 µg/mL, respectively, as shown in Table 3.

3.4. Analysis of anti-colorectal carcinoma, anti-gastric cancer, and anti-pancreatic cancer properties of CLS-CS/Au NPs

The antioxidant effects of recent nanoparticles seem to contribute to their ability to inhibit esophageal cancer in humans. Given the strong connection between tumor progression, oxidative stress, and

inflammation, compounds with antioxidant or anti-inflammatory properties can potentially act as agents to prevent cancer (Beheshtkhoo et al., 2018; Sangami and Manu, 2017). Numerous nanoparticles possess biochemical and pharmacological properties, such as anti-inflammatory and antioxidant effects, which play a role in their anti-carcinogenic and antimutagenic activities (Katata-Seru et al., 2018; Sankar et al., 2014; Namvar et al., 2014; Chen and Schluesener, 2008; Beyene et al., 2017; Radini et al., 2018; Huang et al., 2017; Conde et al., 2012).

Cancer, known for its abnormal cell proliferation and uncontrolled growth, stands as a prominent contributor to mortality. Its development can be attributed to both external factors like chemicals and tobacco, and internal factors like hormones and genetic mutations. To combat this disease, a range of treatment methods including surgery, radiation therapy, and chemotherapy are employed. However, a major challenge lies in delivering targeted drugs to cancer cells without adversely affecting healthy cells, leading to high cancer mortality rates (Huang et al., 2017; Conde et al., 2012; Riehemann et al., 2009; Rai et al., 2014). Nanotechnology appears to offer a promising solution to this issue. The distinctive characteristics of nanoparticles, including their size, surface-to-volume ratio, targeting capabilities, drug-loading capacity for water-insoluble drugs, controlled release mechanisms, and responsiveness to stimuli, position them as viable candidates for cancer therapy (Rai et al., 2014; Jo et al., 2015; Bhattacharya, 2011; Alexander, 2009). When nanoparticles are introduced into the bloodstream, they must traverse the arterial walls to access the desired location and subsequently discharge the medication. Nanoparticles, being larger in size compared to small molecules, are unable to navigate through the narrow gaps between the normal blood vessels endothelial cells. Conversely, the permeable walls of tumor blood vessels facilitate the passage of nanoparticles. Targeted drug administration to the tumor using nanoparticles involves both active and passive targeting mechanisms. Passive targeting leverages the characteristics of the tumor tissue for drug delivery (Radini et al., 2018; Huang et al., 2017; Conde et al., 2012; Riehemann et al., 2009; Rai et al., 2014; Jo et al., 2015). Conversely, the tumor tissue lymphatic system is incomplete and unable to collect nanoparticles and transport them into the bloodstream. In order to achieve passive targeting, the nanoparticles size should generally be below 200 nm. On the other hand, tumor active targeting is accomplished by attaching a ligand such as aptamers, peptides, antibodies, or certain small molecules like folic acid to NPs (Riehemann et al., 2009; Rai et al., 2014; Jo et al., 2015; Bhattacharya, 2011; Alexander, 2009).

The MTT examination was conducted to check the anti-pancreatic cancer, anti-gastric cancer, anti-colorectal carcinoma, and cytotoxicity efficacies of the treated cells with CLS-CS/Au NPs over a 48-hour period on normal (HUVEC) and cancer cells (Fig. 8, 9).

The IC₅₀ values of the CLS-CS/Au NPs were found to be 169 µg/mL for HT-29 (colorectal carcinoma cell), 196 µg/mL for MKN45 (Gastric cancer cell), and 112 µg/mL for PANC-1 (Pancreatic cancer cell). The growth of malignant colorectal, gastric and pancreatic cells was found to decrease in a dose-dependent manner when exposed to CLS-CS/Au NPs (Table 4; Fig. 8, 9).

4. Conclusion

In summary, we have described first time synthesized an eco-friendly material with Au NPs embedded into chitosan-calcium lignosulphonate mixed hydrogel (CLS-CS). The CLS-CS/Au NPs was characterized and applied for reduction of nitroarenes as well. The catalyst remained sufficiently stable to be reused 8 runs without showing a significant drop in activity. The CLS-CS/Au NPs exhibited superior antioxidant properties against DPPH. The IC₅₀ values for the BHT and CLS-CS/Au NPs on DPPH free radicals were 120 and 104 µg/mL, respectively. It appears that the antioxidant effects of these nanoparticles contribute to their anticancer effect. The growth of malignant colorectal, gastric and pancreatic cell lines was found to decrease in a dose-dependent manner

when exposed to CLS-CS/Au NPs. The IC₅₀ values of the CLS-CS/Au NPs were found to be 169 µg/mL for HT-29 (colorectal carcinoma cell), 196 µg/mL for MKN45 (Gastric cancer cell), and 112 µg/mL for PANC-1 (Pancreatic cancer cell).

Funding

Jiangxi Province Science and Technology Department's Surface Project (20224BAB206025).

Project with Jiangxi Provincial Department of Health (202210563).

Declaration of competing interest

The authors declare that they have no known competing financial interests or personal relationships that could have appeared to influence the work reported in this paper.

Acknowledgement

The authors extend their appreciation to the Deanship of Scientific Research at King Khalid University for supporting this work under grant number RGP2/227/44.

References

- (a) Abbasi, N., Ghaneialvar, H., Moradi, R., Zangeneh, M.M., Zangeneh, A., 2021. Arab. J. Chem. 14, 103246. (b) Abdoli, M., Sadrajavadi, K., Arkan, E., Zangeneh, M.M., Moradi, S., Zangeneh, A., Shahlaei, M., Khaledian, S., 2020. J. Drug Deliv. Sci. Technol. 60 (2020), pp. 102044. (c) Gholami, M., Abbasi, N., Ghaneialvar, H., Karimi, E., Afzalnia, A., Zangeneh, M.M., Yadollahi, M., 2022. Nanotechnology, 33, pp. 495603. (d) Jalalvand, A.R., Zangeneh, M.M., Jalili, F., Soleimani, S., Diaz-Cruz, J.M., 2020. Chem. Phys. Lipids 229, 104895.
- Alexander, J.W., 2009. History of the medical use of silver. Surg. Infect. 10, 289–292.
- Allen, T.M., 2002. Ligand-targeted therapeutics in anticancer therapy. Nat. Rev. Cancer 2 (10), 750–763.
- Aromal, S.A., Philip, D., 2012. Green synthesis of gold nanoparticles using Trigonellafoenum-graecum and its size-dependent catalytic activity. Spectrochim. Acta Part A 97, 1–5.
- Ayad, M.M., Amer, W.A., Kotp, M.G., 2017. Mol. Catal. 439, 72–80.
- Beheshthkoo, N., Kouhbanani, M.A.J., Savardashtaki, A., et al., 2018. Green synthesis of iron oxide nanoparticles by aqueous leaf extract of *Daphne mezereum* as a novel dye removing material. Appl. Phys. A 124, 363–369.
- Beyene, H.D., Werkneh, A.A., Bezabeh, H.K., Ambaye, T.G., 2017. Synthesis paradigm and applications of silver nanoparticles (Ag NPs), a review. Sustain. Mater. Technol. 13, 18–23.
- Bhattacharya, S., 2011. Toxicity testing in the 21 century: defining new risk assessment approaches based on perturbation of intracellular toxicity pathways. PLoS ONE. 6, e20887.
- Cermakova, L., Kopecka, I., Pivokonsky, M., et al., 2017. Separ. Purif. Technol. 173, 330–338.
- Chen, X., Schluesener, H.J., 2008. Nanosilver: a nanoparticle in microcosm application. Toxicol. Lett. 176, 1–12.
- Conde, J., Doria, G., Baptista, P., 2012. Noble metal nanoparticles applications in cancer. J. Drug Deliv. 2012, 751075.
- Das, R., Sypu, V.S., Paumo, H.K., Bhaumik, M., Maharaj, V., Maity, A., 2019. Appl. Catal. B: Environ. 244, 546–558.
- Debeaufort, F., Quezada-Gallo, J.A., Voilley, A., 1998. Edible films and coatings: tomorrow's packaging: a review. Crit. Rev. Food Sci. 38 (4), 299–313.
- Fazaeli, R., Aliyan, H., Fazaeli, N., 2010. Open Catal. J. 3, 14–18.
- Fratoddi, I., Cartoni, A., Catone, D., O'Keefe, P., Paladini, A., Toschi, F., Turchini, S., Sciubba, F., Testa, G., Battocchio, C., Carlini, L., Zaccaria, R.P., Magnano, E., Pis, I., Avalidi, L., 2018. Gold nanoparticles functionalized by rhodamine B isothiocyanate to tune plasmonic effects. J. Colloid Interf. Sci. 513, 10–19.
- Gao, J., Wang, Z., Liu, H., Wang, L., Huang, G., 2015. Liposome encapsulated of temozolomide for the treatment of glioma tumor: preparation, characterization and evaluation. Drug Discov Ther. 9 (3), 205–212.
- Guilbert, S., Gontard, N., Gorris, L.G., 1996. Prolongation of the shelf-life of perishable food products using biodegradable films and coatings. LWT-Food Sci. Technol. 29 (1–2), 10–17.
- Huang, Y., Fan, C.Q., Dong, H., Wang, S.M., Yang, X.C., Yang, S.M., 2017. Current applications and future prospects of nanomaterials in tumor therapy. Int. J. Nanomed. 12, 1815–1825.
- Huang, Y., Kang, Y., El-kott, A., Ahmed, A.E., Khames, A., Zein, M.A., 2021. Decorated Cu NPs on Lignin coated magnetic nanoparticles: Its performance in the reduction of nitroarenes and investigation of its anticancer activity in A549 lung cancer cells. Arab. J. Chem. 14, 103299.
- Itani, R., Al Faraj, S.A., 2019. siRNA conjugated nanoparticles-a next generation strategy to treat lung cancer. Int. J. Mol. Sci. 20 (23), 6088.
- Jo, D.H., Kim, J.H., Lee, T.G., Kim, J.H., 2015. Size, surface charge, and shape determine therapeutic effects of nanoparticles on brain and retinal diseases. Nanomed. Nanotechnol. Biol. Med. 11, 1603–1611.
- Katata-Seru, L., Moremedi, T., Aremu, O.S., et al., 2018. Green synthesis of iron nanoparticles using *Moringa oleifera* extracts and their applications: removal of nitrate from water and antibacterial activity against *Escherichia coli*. J. Mol. Liq. 256, 296–304.
- Ledari, R.T., Zhang, W., Radmanesh, M., Mirmohammadi, S.S., Maleki, A., Cathcart, N., Kitaev, V., 2020. Multi-stimuli nanocomposite therapeutic: docetaxel targeted delivery and synergies in treatment of human breast cancer tumor. Small 16, 2002733.
- Li, Y.N., Gu, J., 2014. Recent progress in doxorubicin nano-drug delivery systems for reserving multidrug resistance. 11(3), 177–181.
- Liu, D., Chen, L., Jiang, S., et al., 2014. Formulation and characterization of hydrophilic drug diclofenac sodium-loaded solid lipid nanoparticles based on phospholipid complexes technology. J. Liposome Res. 24 (1), 17–26.
- Lu, Y., Wan, X., Li, L., Sun, P., Liu, G., 2021. Synthesis of a reusable composite of graphene and silver nanoparticles for catalytic reduction of 4-nitrophenol and performance as anti-colorectal carcinoma. J. Mater. Res. Technol. 12, 1832–1843.
- (a) Ma, D., Gong, D., Han, T., Javadi, M., Mohebi, H., Karimian, M., Abbasi, N., Ghaneialvar, H., Zangeneh, M.M., Zangeneh, A., Shahriari, M., Zhang, F., Sun, J., Liu, Y., 2020. Int. J. Biol. Macromol. 165, pp. 767–775. (b) Shi, Z., Mahdavian, Y., Mahdavian, Y., Mahdigholizad, S., Irani, P., Karimian, M., Abbasi, N., Ghaneialvar, H., Zangeneh, A., Zangeneh, M.M., 2022. Arab. J. Chem. 14, pp. 103224. (c) Sun, T., Gao, J., Shi, H., Han, D., Zangeneh, M.M., Liu, N., Liu, H., Guo, Y., Liu, X., 2020. Int. J. Biol. Macromol. 165, pp. 787–795. (d) Zarfashani, H., Mojarab, M., Zangeneh, M. M., Moradipour, P., Bagheri, F., Aghaz, F., Arkan, E., 2022. IEEE Trans. NanoBioscience 21, pp. 520–528.
- Miller, K.S., Krochta, J.M., 1997. Oxygen and aroma barrier properties of edible films: a review. Trends Food Sci. Technol. 8 (7), 228–237.
- Mohammed, M.I., Makky, A.M., Teaima, M.H., Abdellatif, M.M., Hamizawy, M.A., Khalil, M.A., 2016. Transdermal delivery of vancomycin hydrochloride using combination of nano-ethosomes and iontophoresis: in vitro and in vivo study. Drug Deliv. 23 (5), 1558–1564.
- Namvar, F., Rahman, H.S., Mohamad, R., et al., 2014. Cytotoxic effect of magnetic iron oxide nanoparticles synthesized via seaweed aqueous extract. Int. J. Nanomed. 19, 2479–2488.
- Oueslati, M.H., Tahar, L.B., Harrath, A.H., 2020. Catalytic, antioxidant and anticancer activities of gold nanoparticles synthesized by kaempferol glucoside from *Lotus leguminosae*. Arab. J. Chem. 13, 3112–3122.
- Radini, I.A., Hasan, N., Malik, M.A., et al., 2018. Biosynthesis of iron nanoparticles using *Trigonella foenum-graecum* seed extract for photocatalytic methyl orange dye degradation and antibacterial applications. J. Photochem. Photobiol. B 183, 154–163.
- Rai, M., Kon, K., Ingle, A., Duran, N., Galdiero, S., Galdiero, M., 2014. Broad-spectrum bioactivities of silver nanoparticles: the emerging trends and future prospects. Appl. Microbiol. Biotechnol. 98, 1951–1961.
- Riehemann, K., Schneider, S.W., Luger, T.A., Godin, B., Ferrari, M., Fuchs, H., 2009. Nanomedicine—challenge and perspectives. Angew. Chem. 48, 872–897.
- Rossi, A., Donati, S., Fontana, L., Porcaro, F., Battocchio, C., Proietti, E., Venditti, I., Bracci, L., Fratoddi, I., 2016. Negatively charged gold nanoparticles as dexamethasone carrier: stability and cytotoxic activity. RCS Adv. 6, 99016–99022.
- Sangami, S., Manu, M., 2017. Synthesis of Green Iron Nanoparticles using Laterite and their application as a Fenton-like catalyst for the degradation of herbicide Ametryn in water. Environ. Technol. Innov. 8, 150–163.
- Sankar, R., Maheswari, R., Karthik, S., et al., 2014. Anticancer activity of *Ficus religiosa* engineered copper oxide nanoparticles. Mat. Sci. Eng. C 44, 234–239.
- Shah, M.T., Balouch, A., Sirajuddin, A.A., Pathan, A.A., Abdullah, Mahar, A.M., Sabir, S., Khattak, R., Umar, A.A., 2017. Microsyst. Technol. 23, 5745–5758.
- Shahriari, M., Sedigh, M.A., Mahdavian, Y., Mahdigholizad, S., Pirhayati, M., Karmakar, B., Veisi, H., 2021. Int. J. Biol. Macromol. 172, 55–65.
- Shi, Z., Mahdavian, Y., Mahdavian, Y., Mahdigholizad, S., et al., 2021. Cu immobilized on chitosan-modified iron oxide magnetic nanoparticles: Preparation, characterization and investigation of its anti-lung cancer effects. Arab. J. Chem. 14, 103224.
- Singh, P., Pandit, S., Mokkaapati, V.R.S.S., Garg, A., Ravikumar, V., Mijakovic, I., 2018. Gold nanoparticles in diagnostics and therapeutics for human cancer. Int. J. Mol. Sci. 19, 1979.
- Sun, B., Hu, N., Han, L., Pi, Y., Gao, Y., Chen, K., 2019. Anticancer activity of green synthesized gold nanoparticles from *Marsdeniadenacissima* inhibits A549 cell proliferation through the apoptotic pathway. Artif. Cell. Nanomed. B. 47, 4012–4019.
- Trojer, M.A., Li, Y., Wallin, M., Holmberg, K., Nyden, M., 2013. Charged microcapsules for controlled release of hydrophobic actives Part II: surface modification by LbL adsorption and lipid bilayer formation on properly anchored dispersant layers. J. Colloid Interface Sci. 409, 8–17.
- Umamaheswari, C., Lakshmanan, A., Nagarajan, N.S., 2018. Green synthesis, characterization and catalytic degradation studies of gold nanoparticles against Congo red and methyl orange. J. Photochem. Photobiol. B 178, 33–39.
- Veisi, H., Moradi, S.B., Saljoqi, A., Safarimehr, P., 2019. Mater. Sci. Eng. C 100, 445–452.
- Veisi, H., Karmakar, B., Tamoradi, T., Tayebee, R., Sajjadifar, S., Lotfi, S., Maleki, B., Hemmati, S., 2021. Sci. Rep. 11, 1–15.
- Venditti, I., 2019. Engineered gold-based nanomaterials: morphologies and functionalities in biomedical applications. A Mini Review. Bioengineering 6 (2), 53–78.

- Wu, T., Duan, X., Hu, C., Wu, C., Chen, X., Huang, J., Liu, J., Cui, S., 2018. Synthesis and characterization of gold nanoparticles from *Abies spectabilis* extract and its anticancer activity on bladder cancer T24 cells. *Artif. Cell. Nanomed. B.* 47, 512–523.
- Xinli, D.H.Z.S., 2012. Applications of nanocarriers with tumor molecular targeted in chemotherapy. *Chemistry* 75 (7), 621–627.
- Xue, W., Yang, G., Karmakar, B., Gao, Y., 2021. Sustainable synthesis of Cu NPs decorated on pectin modified Fe₃O₄ nanocomposite: Catalytic synthesis of 1-substituted-1H-tetrazoles and in-vitro studies on its cytotoxicity and anti-colorectal adenocarcinoma effects on HT-29 cell lines. *Arab. J. Chem.* 14, 103306.
- Yang, F., Jin, C., Jiang, Y., et al., 2011. Liposome based delivery systems in pancreatic cancer treatment: from bench to bedside. *Cancer Treat. Rev.* 37 (8), 633–642.
- Zhaleh, M., Zangeneh, A., Goorani, S., Seydi, N., Zangeneh, M.M., et al., 2019. In vitro and in vivo evaluation of cytotoxicity, antioxidant, antibacterial, antifungal, and cutaneous wound healing properties of gold nanoparticles produced via a green chemistry synthesis using *Gundeliatournefortii* L. as a capping and reducing agent. *Appl. Organometal. Chem.* 33, e5015 and references cited therein.
- Zhang, W., Veisi, H., Sharifi, R., Salamat, D., Karmakar, B., et al., 2020. Fabrication of Pd NPs on pectin-modified Fe₃O₄ NPs: a magnetically retrievable nanocatalyst for efficient C-C and C-N cross coupling reactions and an investigation of its cardiovascular protective effects. *Int. J. Biol. Macromol.* 160, 1252–1262.
- Zhao, P., El-kott, A., Ahmed, A.E., Khames, A., Zein, M.A., 2021. Green synthesis of gold nanoparticles (Au NPs) using *Tribulus terrestris* extract: investigation of its catalytic activity in the oxidation of sulfides to sulfoxides and study of its anti-acute leukemia activity. *Inorg. Chem. Commun.* 131, 108781.
- Zhou, Y., Zhu, Y., Yang, X., Huang, J., Chen, W., Lv, X., Lia, C., Li, C., 2015. *Rsc. Adv.* 5, 50454–50461.